

SMART: Self-Morphing Anytime Replanning Tree

Zongyuan Shen[†] James P. Wilson[†]Shalabh Gupta^{†*} Ryan Harvey[†]

Abstract—The paper presents an algorithm, called Self-Morphing Anytime Replanning Tree (SMART), that facilitates anytime replanning in dynamic environments. SMART performs risk-based tree-pruning if its current path is obstructed by nearby moving obstacle(s), resulting in multiple disjoint subtrees. Then, for speedy recovery, it exploits these subtrees and performs informed tree-repair at hot-spots that lie at the intersection of subtrees to find a new path. The performance of SMART is comparatively evaluated with seven existing algorithms through extensive simulations. Two scenarios are considered with: 1) dynamic obstacles and 2) both static and dynamic obstacles. The results show that SMART yields significant improvements in replanning time, success rate and travel time. Finally, the performance of SMART is validated by a real laboratory experiment.

Index Terms—Informed replanning, Dynamic environments, Self-repairing trees, Anytime algorithms.

I. INTRODUCTION

Typical path planning problems in a static environment aim to optimize the path between the start and goal states by minimizing a user-specified cost-function (e.g., travel time) [1]. However, many real world applications (e.g., airports, factories, malls, offices, hospitals and homes) consist of moving obstacles (e.g., humans, cobots, carts and wheelchairs). It is envisioned that these applications will be increasingly witnessing the role of cobots in supporting humans for various tasks. Fig. 1 shows a factory environment, where cobots support the basic operations such as supplying raw materials and tools, disposing off scrap, and floor cleaning [2]. It is desired that these cobots autonomously navigate in dynamic environments while replanning in real-time as needed to achieve: 1) high success rates and 2) low travel times.

Replanning strategies are characterized as active or reactive. The active strategies predict the future trajectories of moving obstacles [3] to replan the cobot’s path; however, their performance degrades in crowded environments where these trajectories are difficult to compute, associate and predict [4]. Therefore, the reactive strategies replan the cobot’s path based on the current information. In this regard, this paper presents an algorithm, called Self-Morphing Anytime Replanning Tree (SMART), that facilitates real-time reactive replanning in dynamic environments for uninterrupted navigation.

A. Summary of the SMART Algorithm

To initialize, SMART constructs a search-tree using the RRT* algorithm [5] considering only the static obstacles and finds the initial path. Subsequently, while navigating, the cobot constantly validates its current path for obstructions by nearby

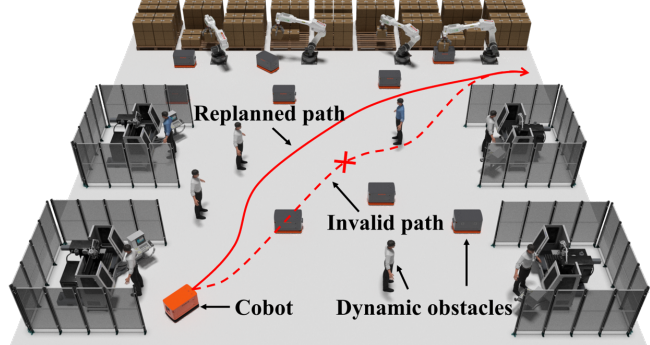


Fig. 1. A factory environment with humans, cobots and machines. dynamic obstacles. If the path is infeasible, SMART performs quick informed replanning that consists of two-steps: 1) tree-pruning and 2) tree-repair. In the tree-pruning step, all risky nodes near the cobot are pruned. This breaks the current tree and forms (possibly) multiple disjoint subtrees. Next, the informed tree-repair step searches for hot-spots that lie at the intersection of different subtrees and provide avenues for real-time tree-repair. Then, the utilities of these hot-spots are computed using the shortest-path heuristics. Finally, these hot-spots are incrementally selected according to their utility for merging disjoint subtrees until a new path is found.

B. Related Work

This section presents a brief literature review of the reactive replanning methods in dynamic environments.

1) *Tree-based Methods*: Several tree-based replanning methods exist based on different tree pruning and repair strategies. Extended RRT (ERRT) [6] removes the entire tree when the current path is obstructed and grows a new tree by biasing samples to the previous path. Dynamic RRT (DRRT) [7] prunes all infeasible nodes and their successors and regrows the goal-rooted tree biased towards the trimmed area. Multipartite RRT (MPRRT) [8] maintains multiple subtrees resulting from node pruning, then reroots the main tree at the cobot’s position and reconnects the disjoint tree roots to the main tree by forest biasing. RRT^X [9] utilizes a graph to explore the area. When the obstacle information changes, it remodels the search-graph by rewiring cascade and repairs a shortest-path-to-goal subtree to find a new path. Horizon-based Lazy RRT* (HLRRT*) [10] checks the path feasibility within a user-defined time-horizon, and prunes all infeasible nodes and their successors resulting in a single tree, then regrows this tree by biasing samples using a Gaussian mixture model (GMM). Efficient Bias-goal Factor RRT (EBGRRRT) [11] prunes the infeasible path nodes and their non-path successors resulting in a main tree rooted at the cobot’s position and a goal tree, then it grows the main tree towards the goal tree. Multi-objective Dynamic RRT* (MODRRT*) [12] connects multiple disjoint tree roots to the goal-rooted tree using feasible straight lines.

[†]Dept. of Electrical and Computer Engineering, University of Connecticut, Storrs, CT 06269, USA.

*Corresponding author (email: shalabh.gupta@uconn.edu)

Distribution A. Approved for public release: distribution unlimited. (AFRL-2023-1595) Date Approved 04-06-2023.

Table I: Comparison of key features of SMART with other tree-based reactive replanning algorithms.

	SMART	ERRT('02) [6]	DRRT('06) [7]	MPRRT('07) [8]	RRT^X('16) [9]	HLRRT*('19) [10]	EBGRRT('20) [11]	MODRRT*('21) [12]
Main Tree Root	Goal	Cobot position	Goal	Cobot position	Goal	Cobot position	Cobot position	Goal
Pruning Strategy	Prunes risky nodes in LRZ. Adds back after replanning	Prunes the entire tree	Prunes all risky nodes and their successors	Prunes all risky nodes	Assigns infinite cost to risky nodes	Prunes all risky nodes and their successors	Prunes risky path nodes and non-path successors	Prunes all risky nodes
Post-pruning Structure	Multiple subtrees	None	Single subtree	Multiple subtrees	Graph	Single subtree	Two subtrees	Multiple subtrees
Replanning Strategy	Reconnects disjoint subtrees at hot-spots in an informed manner	Grows a new tree by sample biasing	Regrows remaining tree by sample biasing	Regrows the main tree by sample biasing	Graph rewiring cascade and repairs shortest-path-to-goal subtree	Regrows remaining tree by sample biasing and lazy collision checking	Regrows the main tree towards goal tree by sample biasing	Reconnects subtree roots to main tree by feasible straight lines
Sampling Strategy	Exploits previous structure; standard sampler if necessary	Waypoint bias, goal bias and standard sampler	Trimmed-area bias, goal bias and standard sampler	Forest bias, goal bias and standard sampler	Standard sampler	GMM-based bias, goal bias and standard sampler	Waypoint bias, goal bias and standard sampler	None

There are several differences between SMART and the aforementioned algorithms. First, most algorithms perform node feasibility checking around all detected dynamic obstacles, except HLRRT* which validates the path in a local user-defined horizon. SMART not only restricts path validation but also tree-pruning to the cobot's neighborhood. Second, some of the above algorithms grow a single (ERRT, DRRT, and HLRRT*) or a double (EBGRRT) tree-structure after pruning, resulting in repeated exploration of the already-explored area. In contrast, SMART leverages on the maximal tree structure with multiple disjoint subtrees which are incrementally merged during replanning. Third, with the exception of MODRRT*, all above algorithms apply standard sampler for replanning, which could lead to wasteful and slow tree growth. In contrast, SMART performs informed tree-repair at hot-spots. Table I shows a comparison of the key features of SMART and other tree-based reactive replanning algorithms.

2) *Probabilistic Roadmap-based Methods*: The main idea is to construct a road map assuming an obstacle-free space and then update it when the obstacle information is available [13]. Both tree-based and probabilistic roadmap based methods have the same time complexity of the processing phase, but the tree-based methods have lower complexity of the query phase, thus making them more suitable for dynamic environments.

3) *Grid-based Methods*: D*-Lite [14] and Lifelong-A* [15] are grid-based replanning algorithms which repair an A*-like solution after edge costs are changed given the updated obstacle information. The grid based methods restrict path planning to the occupancy grid map. In contrast, SMART uses the grid map only to find the hot-spots for tree-repair but plans the path in a continuous space.

4) *Other Methods*: Some optimization-based methods were proposed such as covariant Hamiltonian optimization for motion planning (CHOMP) [16], which use functional gradient techniques to improve the quality of an initial path. Some papers proposed the idea of an escape trajectory as a contingency plan in danger situations [17], [18]. A concept of inevitable collision state was proposed in [19], where a future collision cannot be avoided. In contrast, SMART identifies critical regions where there is a collision risk and deletes the

nodes within. Moreover, velocity obstacle based methods [20] and reinforcement learning based methods [21], [22] have also been proposed for incremental planning.

C. Contributions

The paper makes the following contributions:

- Development of the SMART algorithm based on fast informed-replanning for real-time dynamic environments.
- Comprehensive comparison to existing algorithms.
- Validation using simulation and experimental tests.

D. Organization

The remainder of this paper is organized as follows. Section II presents the details of SMART algorithm and Section III provides the algorithm analysis. Section IV shows the simulation and experimental results. Finally, Section V concludes the paper with recommendations for future work.

II. SMART ALGORITHM

Let $\mathcal{X} \subset \mathbb{R}^2$ be a region populated by both static and dynamic obstacles. Let $\mathcal{X}_N \subset \mathcal{X}$ be the navigation space free of static obstacles. Let $\mathcal{O} = \{O_i : i = 1, 2, \dots, m\}$ be the set of m dynamic circular obstacles, where $r_i \in \mathbb{R}^+$ is the radius of obstacle $O_i \in \mathcal{O}$, and $x_i(t) \in \mathcal{X}_N$ and $v_i(t) \in \mathbb{R}^+$ denote its position and speed at time $t \in \mathbb{R}^+$, respectively. Let \mathcal{R} be a circular cobot of radius $r_{\mathcal{R}} \in \mathbb{R}^+$, where $x_{\mathcal{R}}(t) \in \mathcal{X}_N$ and $v_{\mathcal{R}}(t) \in \mathbb{R}^+$ denote its position and speed at time t , respectively. Let (x_s, x_g) denote the start and goal positions.

A. Initialization

First, a tiling is constructed on the space \mathcal{X} as defined below.

Definition II.1 (Tiling). A set $\mathcal{C} = \{c_j \subset \mathbb{R}^2 : j = 1, \dots, |\mathcal{C}|\}$, is a tiling of \mathcal{X} , if its elements, called tiles (or cells), have mutually exclusive interiors and cover \mathcal{X} , i.e.,

- $c_j^o \cap c_{j'}^o = \emptyset, \forall j, j' \in \{1, \dots, |\mathcal{C}|\}, j \neq j'$

- $\mathcal{X} \subseteq \bigcup_{j=1}^{|\mathcal{C}|} c_j$,

where c_j^o denotes the interior of cell $c_j \in \mathcal{C}$.

Note: The tiling is used only for searching hot-spots (Section II-C). The planning and navigation happens in \mathcal{X}_N .

SMART is initialized by constructing a RRT* [5] tree $\mathcal{T}^0 = (\mathcal{N}^0, \mathcal{E}^0)$ rooted at the goal x_g , where $(\mathcal{N}^0, \mathcal{E}^0)$ denote the sets

of nodes and edges. The tree is created such that each cell of the tiling has at least one node. Each of these nodes maintain a data structure including the information about its position, parent, children, tree index, cell index and node status as active or pruned. Initially, all nodes are marked active. Then an initial path is found using \mathcal{T}^0 . The path is time embedded to produce the initial trajectory $\sigma^0 : [t_0, t_f] \rightarrow \mathcal{X}_N$, which is a continuous and bounded function, s.t. $\sigma^0(t_0) = x_s$ and $\sigma^0(t_f) = x_g$. As the cobot moves, σ^0 could be blocked by dynamic obstacles \mathcal{O} . Thus, the paper presents an informed replanning strategy consisting of two-steps: 1) tree-pruning and 2) tree-repair.

B. Tree-Pruning

To find a safe trajectory via replanning, it is important to identify and prune the risky nodes of the tree. Since: 1) dynamic obstacles far away from the cobot do not pose an immediate risk, and 2) it is computationally inefficient to perform feasibility checking around all detected obstacles, the paper presents a local tree-pruning (LTP) strategy described below. First, we define the following.

Definition II.2 (Local Reaction Zone). A local reaction zone (LRZ) is defined for the cobot \mathcal{R} , such that $LRZ_{\mathcal{R}}(t) = \{x \in \mathcal{X}_N : \|x - x_{\mathcal{R}}(t)\| \leq v_{\mathcal{R}}(t) \times T_{RH} + r_{\mathcal{R}}\}$, where $T_{RH} \in \mathbb{R}^+$ is the reaction time-horizon.

Definition II.3 (Obstacle Hazard Zone). An obstacle hazard zone (OHZ) is defined for each dynamic obstacle $O_i \in \mathcal{O}$, such that $OHZ_i(t) = \{x \in \mathcal{X}_N : \|x - x_i(t)\| \leq v_i(t) \times T_{OH} + r_i\}$, where $T_{OH} \in \mathbb{R}^+$ is the obstacle risk time-horizon.

Definition II.4 (Critical Pruning Region). Let \mathcal{D} denote all the obstacles that are intersecting with LRZ and pose danger to the cobot such that $\mathcal{D} = \{\mathcal{O}_i : LRZ_{\mathcal{R}}(t) \cap OHZ_i(t) \neq \emptyset\}$. Then, the critical pruning region (CPR) is defined as

$$CPR(t) = \bigcup_{\mathcal{D}} OHZ_i(t). \quad (1)$$

Fig. 2 shows the LTP strategy. The cobot constantly checks the validity of its current path by checking the path nodes and edges in LRZ starting from its current position. According to the LTP strategy, if the current path is invalid, then all tree portions that fall within CPR are considered to be risky for the replanned path and are pruned. If a node is invalid, it is pruned along with its edges. If an edge is invalid but its two end nodes are safe, then only this edge is pruned. The parent and child information of all affected nodes is updated. Tree-pruning could break the current tree \mathcal{T} into disjoint subtrees.

Definition II.5 (Disjoint Subtree). A *disjoint subtree* is a portion of the current tree T whose root is either a child of a pruned node or the goal.

Let $\mathcal{T}_0, \mathcal{T}_1, \dots, \mathcal{T}_{K-1}$ be the $K \in \mathbb{N}^+$ disjoint subtrees formed after pruning, where \mathcal{T}_0 is the subtree rooted at the goal. Similarly, let \mathcal{N}^a and \mathcal{N}^p be the sets of alive and pruned nodes, respectively, such that $\mathcal{N}^0 = \mathcal{N}^a \cup \mathcal{N}^p$.

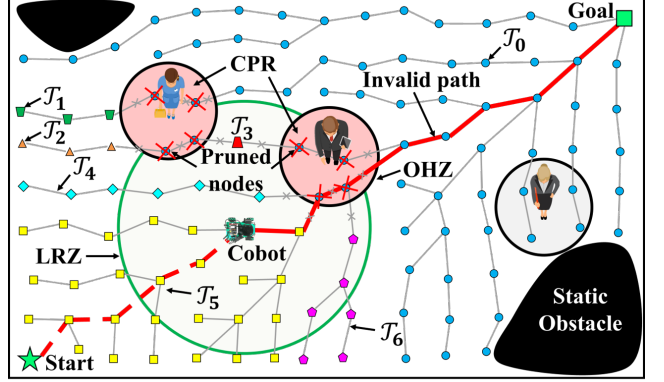


Fig. 2. Illustration of the local tree pruning strategy.

C. Tree-Repair

The tree-pruning step is followed by the tree-repair step, which is done to find an updated path to the goal. Let t_u be the time instant at which the current path is blocked and the objective is to find an updated safe trajectory $\sigma : [t_u, t_f'] \rightarrow \mathcal{X}_N \setminus CPR(t_u)$, s.t. $\sigma(t_u) = x_R(t_u)$ and $\sigma(t_f') = x_g$.

Fig. 3 shows an example of the tree-repair process. For fast and efficient tree-repair, SMART exploits the previous exploration efforts by retaining all the disjoint subtrees and pruned nodes for possible future additions. Thus, SMART searches for hot-spots on disjoint subtrees for tree-repair.

1) *Search for Hot-Spots*: The search begins in the vicinity of the damaged path. Thus, the following is defined.

Definition II.6 (Local Search Region). Let $\hat{n} \in \mathcal{N}^p$ be the pruned path node which is closest to the cobot. Let $c_{\hat{n}} \in \mathcal{C}$ be the cell containing \hat{n} . Then, the local search region (LSR) is defined as the $\ell \times \ell$ neighborhood $\mathcal{S}^\ell \subseteq \mathcal{C}$ of $c_{\hat{n}}$, $\ell \in 2\mathbb{N}^+ + 1$.

The search starts in \mathcal{S}^ℓ , $\ell = 3$. It is a two-step process.

a) *Identifying Disjoint Subtrees*: The first step is to identify and label the disjoint subtrees in \mathcal{S}^ℓ (Fig. 3a). To do this, an unlabeled node $n \in \mathcal{N}^a$ is picked within \mathcal{S}^ℓ and assigned a tree index $k \in \{0, \dots, K-1\}$, where index 0 corresponds to the goal rooted subtree. Then it is backtracked while labeling all ancestor nodes with the same tree index until reaching either 1) the unlabeled subtree root or 2) a labeled ancestor (or root) from a previous backtracking. In the second case, all nodes visited during backtracking are labeled with the same tree index as that of this ancestor. The above process is repeated until all nodes inside \mathcal{S}^ℓ are labeled with their tree-indices.

b) *Identifying Hot-Spots:* A hot-spot is defined as follows.

Definition II.7 (Hot-Spot). A cell $c \in \mathcal{S}^\ell$ is a hot-spot if:

1. *it contains nodes of a) at least two disjoint subtrees, or b) a single subtree and at least one of its neighboring cell contains nodes of another disjoint subtree, and*
2. *the edge connecting at least one node pair corresponding to two disjoint subtrees in 1.a) or 1.b) above is feasible.*

Thus, the regions where disjoint subtrees intersect form hot-spots for fast and easy tree-repair. To identify hot-spots, a hot-spot map is constructed on \mathcal{S}^ℓ based on Defn. II.7 as follows.

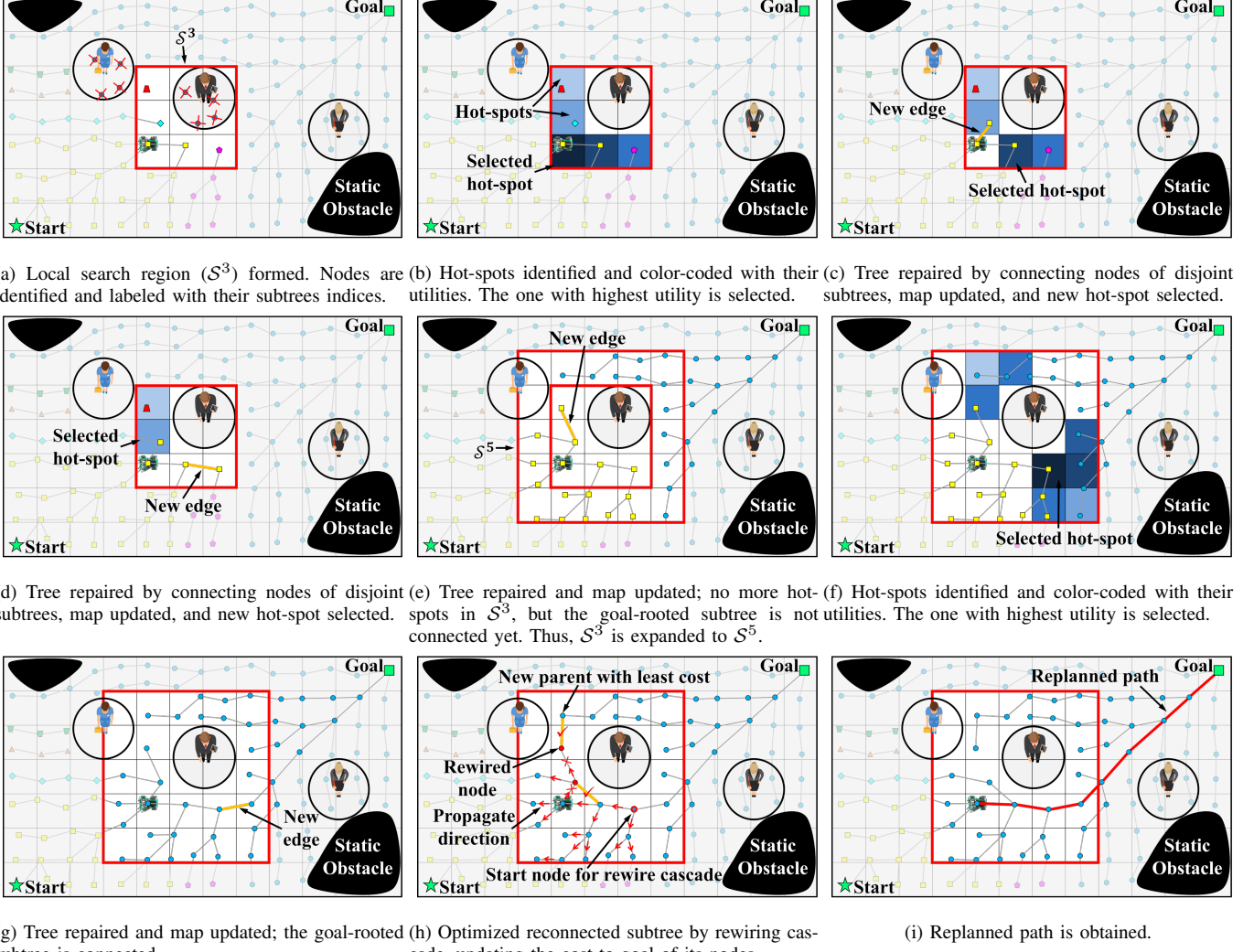


Fig. 3. Illustration of the Tree-Repair Step.

Definition II.8 (Hot-Spot Map). A hot-spot map is defined on \mathcal{S}^ℓ such that $h^\ell : \mathcal{S}^\ell \rightarrow \{1, -1\}$, where 1, -1 denote hot-spot and not a hot-spot, respectively.

Let $\mathcal{H}^\ell \subset \mathcal{S}^\ell$ denote the set of all hot-spots in \mathcal{S}^ℓ (Fig. 3b). If no hot-spot is found within \mathcal{S}^ℓ , s.t. $h^\ell(c) = -1, \forall c \in \mathcal{S}^\ell$, then the search area is expanded to size $\ell = \ell + 2$ and steps a) and b) are repeated until at least one hot-spot is found.

2) *Ranking of the Hot-Spots:* Once all hot-spots are detected in the LSR, they are ranked using a utility map (Fig. 3b).

Definition II.9 (Utility Map). A utility map is defined on \mathcal{H}^ℓ such that $\mathcal{U}^\ell : \mathcal{H}^\ell \rightarrow \mathbb{R}^+$, where the utility of a cell $c \in \mathcal{H}^\ell$ is computed as follows

$$\mathcal{U}^\ell(c) = \begin{cases} \frac{\alpha}{\|x_{\mathcal{R}}(t_u) - p_c\|_2 + \min_{n_i \in \mathcal{N}_c \cap \mathcal{N}_0} g(n_i)} & \text{if } \mathcal{N}_c \cap \mathcal{N}_0 \neq \emptyset \\ \frac{1}{\|x_{\mathcal{R}}(t_u) - p_c\|_2 + \|p_c - x_g\|_2} & \text{else,} \end{cases} \quad (2)$$

where $p_c \in \mathbb{R}^2$ is the centroid of cell c ; $\mathcal{N}_c \subset \mathcal{N}^a$ is the set of alive nodes inside c ; $\mathcal{N}_0 \subset \mathcal{N}^a$ is the set of nodes

Distribution A. Approved for public release: distribution unlimited. (AFRL-2023-1595) Date Approved 04-06-2023.

of the goal-rooted subtree \mathcal{T}_0 ; $g(n_i)$ returns the travel cost from node n_i to the goal via the shortest path on \mathcal{T}_0 ; and $\alpha > 1$ is a bias factor used to encourage rewiring with \mathcal{T}_0 . In summary, if the hot-spot contains a node of \mathcal{T}_0 , then its utility is determined by the heuristic cost-to-cobot and the actual cost-to-goal; otherwise, it is given by the total heuristic cost.

3) *Tree-Repairing:* This consists of the following steps:

- Pick the hot-spot with the highest utility (Figs. 3b-3d and 3f). (If there is no hot-spot in \mathcal{S}^ℓ after tree-repairing, then $\ell = \ell + 2$ and go back to II-C1 (Fig. 3e)).
- Pick an unexamined node from the selected hot-spot. (If all nodes have been examined, then go back to a.)
- Pick an unexamined node belonging to a different subtree from the selected hot-spot or its local neighborhood. (If all nodes from different subtrees have been examined, then go back to step b.)
- Connect the above node-pair if the edge is feasible (Figs. 3c-3e and 3g); otherwise, go back to step c.)
- Update the parent-child relationships and subtree indices (Figs. 3c-3e and 3g): 1) if any node from the node-pair above belongs to \mathcal{T}_0 , then this node is set as the parent and all nodes of the connected subtree in \mathcal{S}^ℓ are assigned

the index of \mathcal{T}_0 and their cost-to-goal are updated, or 2) if none of the nodes in the node-pair belongs to \mathcal{T}_0 , then the selected node is set as the parent and all nodes of the connected subtree in \mathcal{S}^ℓ are assigned its index. A change in a node's parent is propagated to all its ancestors.

f. Update the hot-spot and utility maps (Figs. 3c-3e and 3g).
g. Check if \mathcal{T}_0 is reachable from $x_{\mathcal{R}}$ (Fig. 3g). If true, then a path can be found to the goal; otherwise, go back to c.

Remark 1. If the entire space is exhausted by informed tree-repair and it is found that no path exists using alive samples, then a random sampling and repairing process is started to guarantee probabilistic completeness.

D. Tree-Optimization and Path Search

During tree-repair, several subtrees were connected to ultimately merge with \mathcal{T}_0 . These subtrees are optimized using rewiring cascade [9] starting from all subtree nodes \mathcal{N}_s connected to \mathcal{T}_0 (Fig. 3h). Then, an updated trajectory σ is found using \mathcal{T}_0 (Fig. 3i). After that, all nodes in \mathcal{N}^p and the roots of the remaining disjoint trees are reconnected with \mathcal{T}_0 and a single tree \mathcal{T} is formed. While navigating σ , rewiring cascade is run once from the root of \mathcal{T} excluding the dynamic obstacles to prepare for the next replanning incident. Algorithm 1 describes the functioning of SMART.

III. ALGORITHM ANALYSIS

Let \mathcal{W} denote the minimal cover of the CPR using the tiling \mathcal{C} . Let $\mathcal{N}_{\mathcal{W}}$ be the set of all nodes in \mathcal{W} s.t. $\mathcal{N}^p \subseteq \mathcal{N}_{\mathcal{W}} \subseteq \mathcal{N}^0$. Let $\bar{n} \geq 1$ be the average number of nodes per cell. Let h be the average number of neighbors of each node. Let $S^{\tilde{\ell}}, \tilde{\ell} \leq \ell_{max}$, be the smallest LSR where sufficient hot-spots are found to connect the cobot to \mathcal{T}^0 .

Lemma III.1. The tree-pruning complexity is $O(|\mathcal{N}_{\mathcal{W}}|)$.

Proof. For tree-pruning, the first step is to identify the CPR for $|\mathcal{D}|$ obstacles that intersect with the LRZ; this has a complexity of $O(|\mathcal{D}|)$. Next, \mathcal{W} is determined by querying cells using the obstacle locations in the CPR ; this has a complexity of $O(|\mathcal{W}|)$. Then, the nodes falling inside the \mathcal{W} cells are queried from a data structure and checked for feasibility; this has a complexity of $O(2|\mathcal{N}_{\mathcal{W}}|)$. Since SMART uses a search tree, there are at most $|\mathcal{N}_{\mathcal{W}}|$ edges that need to be checked; this has a complexity of $O(|\mathcal{N}_{\mathcal{W}}|)$. Thus, the overall complexity is $O(3|\mathcal{N}_{\mathcal{W}}| + |\mathcal{W}| + |\mathcal{D}|)$. Since $|\mathcal{N}_{\mathcal{W}}| \geq |\mathcal{W}| \geq |\mathcal{D}|$, the overall complexity of tree-pruning is $O(|\mathcal{N}_{\mathcal{W}}|)$. \square

Lemma III.2. The tree-repair complexity is $O(|\mathcal{N}^0| + h\bar{n}|\mathcal{S}^{\tilde{\ell}}|)$.

Proof. The first step in tree-repair is to label each node in \mathcal{S}^ℓ by backtracking, which has a worst-case complexity of $O(|\mathcal{N}^0 \setminus \mathcal{N}^p|) \leq O(|\mathcal{N}^0|)$. The next step is to find the sufficient set of hot-spots for tree-repair. The hot-spot status of any cell $c \in \mathcal{S}^\ell$ is checked by comparing the subtree indices of each node in c with up to h neighboring nodes in \mathcal{S}^ℓ (Defn. II.7-1). For \bar{n} nodes per cell, this has a complexity of $O(h\bar{n})$ per cell. Then, the feasibility of the

Algorithm 1: SMART

```

1  $\{\mathcal{T}^0, \sigma^0\} \leftarrow \text{RRT}^*(x_s, x_g, \mathcal{X}_N)$ ; // initialization
2  $t = t_0, \mathcal{T} = \mathcal{T}^0, \sigma = \sigma^0$ ;
3 while  $x_{\mathcal{R}} \neq x_g$  do // goal unreached
4    $t \leftarrow \text{UpdateClock}()$ ;
5    $\{x_i(t), v_i(t)\}_{i=1..m} \leftarrow \text{UpdateObstacleState}()$ ;
6    $\{x_{\mathcal{R}}(t), v_{\mathcal{R}}(t)\} \leftarrow \text{UpdateCobotState}()$ ;
7   if  $\text{ValidatePath}(\sigma, LRZ_{\mathcal{R}}(t), \{OHZ_i(t)\}_{i=1..m})$  then
8     Navigate( $\sigma$ );
9   else
10     $\sigma \leftarrow \text{void}$ ; // invalid path
11     $\{\mathcal{T}_0, \dots \mathcal{T}_{K-1}\} \leftarrow \text{TreePruning}(\mathcal{T}, CPR(t))$ ; // II-B
12     $\ell \leftarrow 1, \mathcal{H}^\ell \leftarrow \emptyset, \mathcal{N}_s \leftarrow \emptyset$ ; // initialize repair
13    while  $\mathcal{T}_0$  is not reachable from  $x_{\mathcal{R}}$  do
14      if  $\ell < \ell_{max}$  then // informed tree-repair
15         $\ell \leftarrow \ell + 2$ ;
16         $\mathcal{H}^\ell \leftarrow \text{HotSpotSearch}(\mathcal{S}^\ell)$ ; // II-C1
17         $\mathcal{U}^\ell \leftarrow \text{ComputeUtility}(\mathcal{H}^\ell)$ ; // II-C2
18         $\{\mathcal{N}_s, \mathcal{T}_0\} \leftarrow \text{TreeRepair}(\mathcal{U}^\ell, \mathcal{S}^\ell)$ ; // II-C3
19      else // standard tree-repair
20         $x_{rand} \leftarrow \text{SampleFree}()$ ;
21        Join  $x_{rand}$  to all nearby reachable subtrees;
22        if  $x_{rand} \in \mathcal{T}_0$  then Rewire( $x_{rand}$ );
23      end
24    end
25     $\mathcal{T}_0 \leftarrow \text{TreeOptimization}(\mathcal{T}_0, \mathcal{N}_s)$ ; // II-D
26     $\sigma \leftarrow \text{PathSearch}(x_{\mathcal{R}}, x_g, \mathcal{T}_0)$ ; // II-D
27    Add  $\mathcal{N}^p$  and disjoint subtrees to  $\mathcal{T}_0$  to get a single tree  $\mathcal{T}$ ;
28  end
29 end

```

corresponding edges is checked (Defn. II.7-2). This has a complexity of $O(h\bar{n})$ per cell. Thus, the complexity to check the hot-spot status of a cell is $O(2h\bar{n}) = O(h\bar{n})$. During the expansion of \mathcal{S}^ℓ , it becomes clear with little investigation that the hot-spot status of a cell is checked a maximum of two times. Thus, the complexity to find the sufficient hot-spots is $O(2h\bar{n}|\mathcal{S}^{\tilde{\ell}}|) = O(h\bar{n}|\mathcal{S}^{\tilde{\ell}}|)$. Next, the complexity of computing utilities for $|\mathcal{S}^{\tilde{\ell}}|$ cells (a cell can be a hot-spot up to two times) is $O(2|\mathcal{S}^{\tilde{\ell}}|) = O(|\mathcal{S}^{\tilde{\ell}}|)$. Finally, tree-repair is done via node reconnections. Similar to the hot-spot search, this step finds all neighboring nodes that belong to different subtrees and have a feasible connecting edges. This has a complexity of $O(h\bar{n})$ per hot-spot. For $|\mathcal{S}^{\tilde{\ell}}|$ cells that could each be a potential hot-spot up to two times, this step has a complexity of $O(2h\bar{n}|\mathcal{S}^{\tilde{\ell}}|) = O(h\bar{n}|\mathcal{S}^{\tilde{\ell}}|)$. Thus, the overall complexity of tree-repair is $O(|\mathcal{N}^0| + (2h\bar{n} + 1)|\mathcal{S}^{\tilde{\ell}}|) = O(|\mathcal{N}^0| + h\bar{n}|\mathcal{S}^{\tilde{\ell}}|)$. \square

Lemma III.3. The tree-optimization complexity is $O(h|\mathcal{N}^0|)$.

Proof. In the worst-case scenario, the subtree \mathcal{T}_0 initially contained only the goal node, and all disjoint subtrees $\mathcal{T}_1, \dots, \mathcal{T}_{K-1}$ were reconnected to \mathcal{T}^0 during tree-repairing. Thus, the rewiring cascade must propagate through $|\mathcal{N}^0| - 1$ nodes. Since there are h neighbors per node, the overall complexity for tree-optimization is $O(h(|\mathcal{N}^0| - 1)) = O(h|\mathcal{N}^0|)$. \square

Theorem 1. The complexity of SMART is $O(h|\mathcal{N}^0|)$.

Proof. From Lemmas III.1-III.3, the complexity is $O(|\mathcal{N}_{\mathcal{W}}| + h\bar{n}|\mathcal{S}^{\tilde{\ell}}| + (h+1)|\mathcal{N}^0|)$. Since $|\mathcal{N}_{\mathcal{W}}| \leq |\mathcal{N}^0|$ and $\bar{n}|\mathcal{S}^{\tilde{\ell}}| \leq |\mathcal{N}^0|$, the complexity reduces to $O(h|\mathcal{N}^0|)$. \square

Theorem 2. SMART informed replanner is complete with respect to the sample-based representation of the environment.

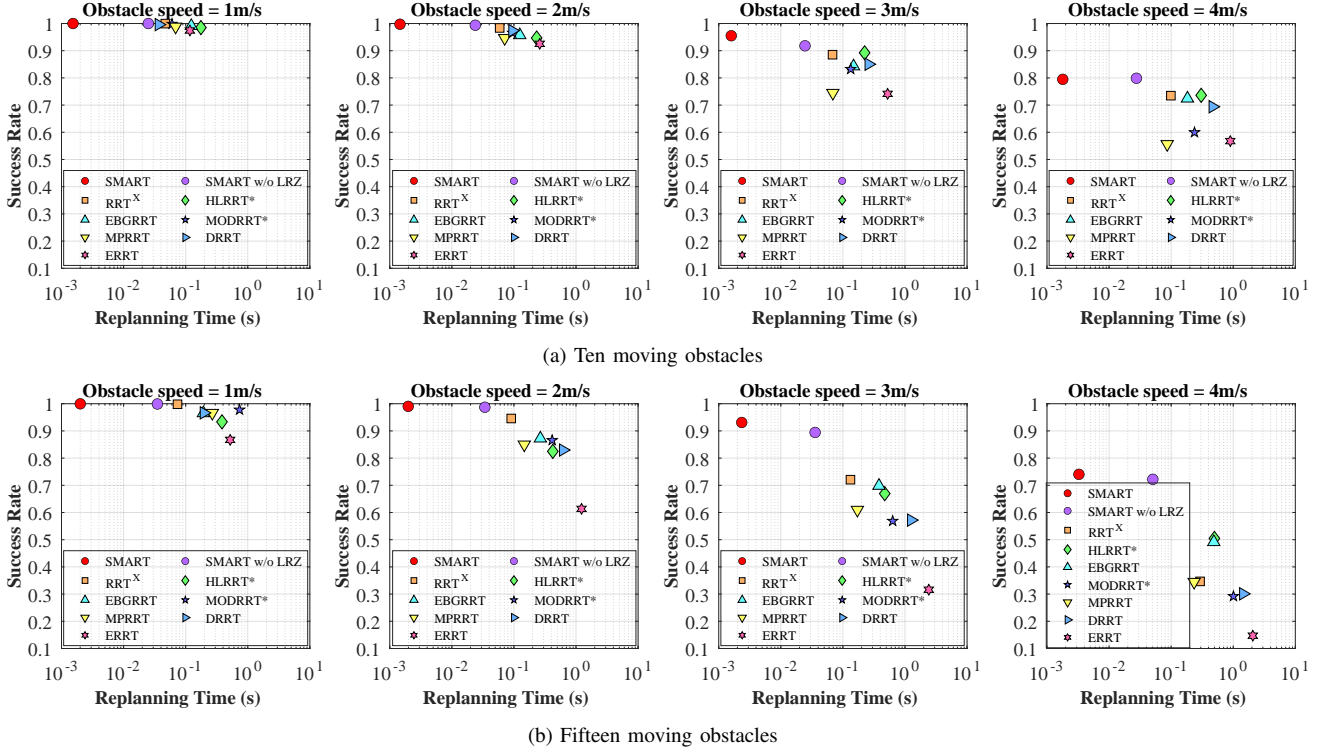


Fig. 4. Average replanning time and success rate for randomly generated scenarios.

Proof. If a path exists using alive nodes \mathcal{N}^a , then by Defn. II.7 the hot-spot nodes are necessary and sufficient for replanning. While the incremental hot-spot search guarantees that all hot-spots will be found, the tree-repair sequentially merges and relabels all adjacent subtrees at hot-spots. This guarantees that the cobot will be eventually connected to the goal-rooted tree \mathcal{T}_0 and a path is found. \square

IV. RESULTS AND DISCUSSION

This section presents the testing and validation results of the SMART algorithm via: 1) simulation studies on scenarios containing a) dynamic obstacles and b) both static and dynamic obstacles, and 2) real-experiments in a laboratory.

A. Validation by Simulation Experiments

The performance of SMART is comparatively evaluated with existing methods (Table I) by extensive simulations.

1) *Simulation Set-Up:* SMART is implemented on a holonomic cobot of radius $0.5m$ that moves at a speed of $v_R = 4m/s$. The simulations include dynamic obstacles of radius $0.5m$ that move along a random heading from $[0, 2\pi]$ for a random distance from $[0, 10m]$ before changing their heading. Upon hitting the border of space, a new heading and moving distance are selected. Two different scenarios are considered:

- *Scenario 1 with Dynamic Obstacles:* This scenario consists of a $32m \times 32m$ space populated with only dynamic obstacles. Two cases are conducted including a) 10 and b) 15 obstacles. Each obstacle moves at the same speed selected from the set $\{1, 2, 3, 4\}m/s$, resulting in 8 different combinations of the number of obstacles and speeds. For each

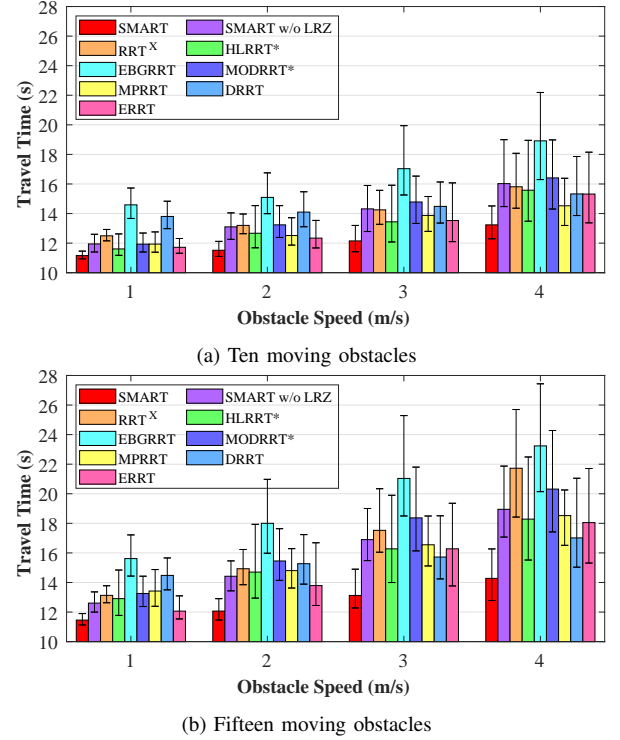


Fig. 5. Travel times of successful trials showing the median value and the 25th and 75th percentiles.

combination, 30 different obstacle trajectories are generated to intersect the cobot, resulting in a total of 240 case studies.

- *Scenario 2 with Static and Dynamic Obstacles:* This scenario depicts a real situation (e.g., a factory) with both static and dynamic obstacles (Fig. 6a). It consisted of a $66m \times 38m$ space with a static obstacle layout and 10 dynamic obstacles. Each obstacle moves at a different speed selected from the

set $\{1, 2, 3, 4\} \text{m/s}$. Then, 30 different obstacle trajectories are generated to intersect the cobot, resulting in 30 case studies.

For each scenario above, 100 trials are performed for each of the aforementioned cases studies for each algorithm. All algorithms were deployed in C++ and run on a computer with 2.60 GHz processor and 32 GB RAM. For the same trial, a fixed random seed is used for random sample generation for all algorithms, and their initial search trees are of the same size. A trial is marked as failed and the travel time is not recorded if the cobot collides with any obstacle. For SMART, the tiling was generated with cell size of $1\text{m} \times 1\text{m}$. The reaction time-horizon was set as $T_{RH} = 0.8\text{s}$. An obstacle risk time-horizon of $T_{OH} = 0.4\text{s}$ is added to all dynamic obstacles for all algorithms. If the cobot moves into an OHZ, then the OHZ is ignored but the actual obstacle is considered for collision checking. The goal bias and random sample rates shared by most algorithms (except RRT^X and MODRRT^{*}) are set based on [10] as 0.1 and 0.2 respectively. All other algorithm-specific parameters are set based on the corresponding papers.

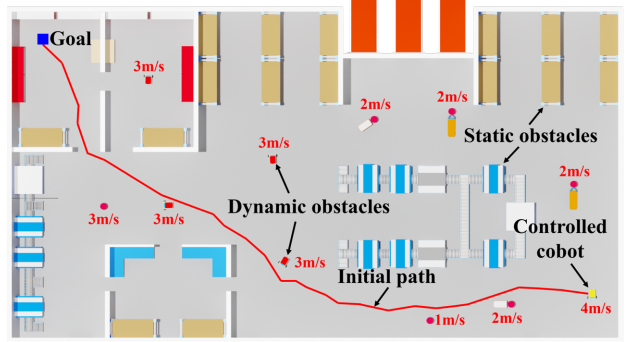
To consider sensor uncertainties, noise was injected into the range, the heading angle, and the position of cobot during simulation. A typical lidar (e.g., RPLIDAR S2L [23]) provides an accuracy of 0.03m , and a modestly priced compass can provide an accuracy of 1° [24]. Based on these, the uncertainties were simulated as uniform distributions $U_{[-0.03\text{m}, 0.03\text{m}]}$ and $U_{[-1^\circ, 1^\circ]}$ for range and heading, respectively. Similarly, an indoor localization system (e.g., Hagisonic StarGazer) provides a precision of 0.02m [25]. Thus, the localization uncertainty is simulated as a uniform distribution $U_{[-0.02\text{m}, 0.02\text{m}]}$.

2) Performance Metrics: The following metrics are considered for comparative performance evaluation:

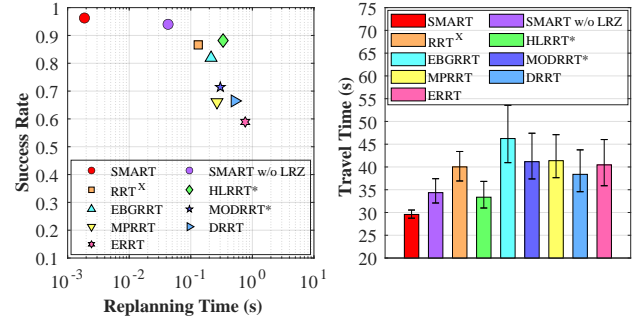
- Replanning time: Time to replan a new path.
- Success rate: Fraction of successful runs out of the total.
- Travel time: Time from start to goal without collision.

3) Simulation Results: Fig. 4 shows the comparative evaluation results on Scenario 1. Overall, SMART achieves significant improvements over other algorithms in success rate and replanning time in all case studies. This follows from the facts that i) tree-pruning not only reduces collision checking to nearby obstacles but also produces less number of disjoint trees for repairing, and ii) tree-repair exploits the disjoint subtrees and facilitates repairing at hot-spots for speedy recovery. Fig. 5 shows that SMART achieves the lowest travel times because of i) lowest replanning time and ii) infrequent replanning. Furthermore, to investigate the value of the tree-repair step, we present an ablation study, where LRZ is removed, thus pruning all risky nodes. Fig. 4 and Fig. 5 show that SMART w/o LRZ still performs significantly better than all other algorithms in replanning time and success rate.

• Effect of Obstacle Speed: As seen in Fig. 4, while the replanning time of SMART is minimally affected by obstacle speed, the success rate dips when obstacle speed is greater than 2m/s . This is because high-speed moving obstacles have higher chance to hit the cobot. Moreover, as shown in Fig. 5,



(a) Simulated factory environment.



(b) Simulation result.

Fig. 6. Simulation results of a factory environment.

the travel time goes up with the obstacle speed because high-speed obstacles cause frequent replannings.

• Effect of Obstacle Number: As seen in Fig. 4, the replanning time increases slightly with an increase in obstacle number because of i) more disjoint subtrees for repairing and ii) more complex environment with smaller free space. The success rate dips with an increase in obstacle number for high obstacle speed because longer replanning time and crowded environment increase collision probability. Similarly, as shown in Fig. 5, the travel time goes up with the obstacle number because of frequent replannings and complex environment.

Fig. 6b shows the same trend in Scenario 2. As seen, SMART outperforms all other methods in terms of replanning time, success rate, and the total travel time.

B. Validation by Real Experiments

The SMART algorithm is further validated by real experiments in a $7\text{m} \times 7\text{m}$ lab space with both static and dynamic obstacles. A cobot called ROSMASTER X3 [23] is used that is equipped with 1) a RPLIDAR S2L lidar [23] with a range of 8m for obstacle detection, 2) MD520 motor with encoder [23] for detection of rotation angle and linear displacement, and 3) MPU9250 IMU [23] for detection of speed, acceleration, and orientation. An Extended Kalman Filter [26] is used to fuse data from the IMU and motor encoder for localization. The space is tiled with $0.1\text{m} \times 0.1\text{m}$ cells. The occupancy grid mapping algorithm [27] is used offline to create a static obstacle map, while the humans are detected in real-time. The cobot carries Jetson Nano minicomputer that collects sensor measurements and runs the SMART algorithm for real-time replanning, control and navigation. Fig. 7 shows the various snapshots of an experiment, where the cobot successfully replans a new path multiple times to avoid obstacles until

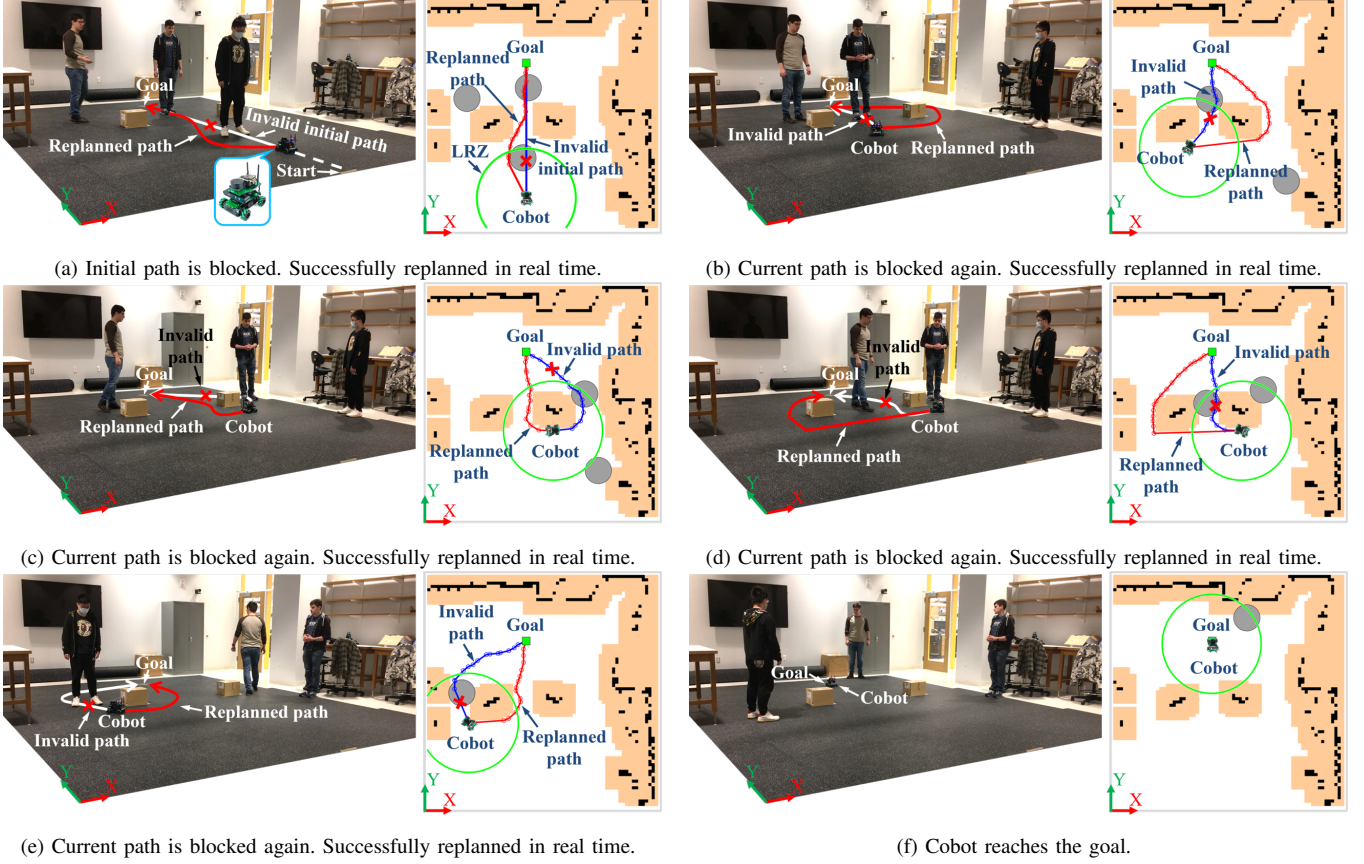


Fig. 7. Snapshots of a real experiment in a laboratory with both static and dynamic obstacles.

reaching the goal, thus revealing the effectiveness of SMART. The observed replanning time is $\sim 0.03s$.

V. CONCLUSIONS AND FUTURE WORK

The paper presents an algorithm, called SMART, for anytime replanning in dynamic environments. To replan a path, SMART performs risk-based tree-pruning to form multiple disjoint subtrees, then exploits and repairs them at selected hot-spots for speed recovery. It is shown that SMART is computationally efficient and complete. The comparative evaluation with existing algorithms shows that SMART significantly improves the replanning time, success rate, and travel time. Finally, SMART is validated by real experiments.

With further research and investigation, SMART has the potential for extending to non-holonomic robots [28], [29] and higher dimensional problems. The challenges include 1) defining configuration space including the rotational space components, 2) identifying efficient strategies for partitioning and sampling in the configuration space, and 3) considering the motion constraints in the cost functions, tree reconnections and the initial tree construction. Further SMART could be extended to problems with 1) joint time-risk optimization, 2) multi-cobot systems [30], and 3) coverage path planning [31], [32].

Distribution A. Approved for public release: distribution unlimited. (AFRL-2023-1595) Date Approved 04-06-2023.

REFERENCES

- [1] J. Song, S. Gupta, and T. A. Wettergren, “T*: Time-optimal risk-aware motion planning for curvature-constrained vehicles,” *IEEE Robot. Automat. Lett.*, vol. 4, no. 1, pp. 33–40, 2019.
- [2] J. Song and S. Gupta, “e*: An online coverage path planning algorithm,” *IEEE Trans. Robot.*, vol. 34, pp. 526–533, 2018.
- [3] J. Wang, M. Q.-H. Meng, and O. Khatib, “EB-RRT: Optimal motion planning for mobile robots,” *IEEE Trans. Autom. Sci. Eng.*, vol. 17, no. 4, pp. 2063–2073, 2020.
- [4] J. Z. Hare, J. Song, S. Gupta, and T. A. Wettergren, “Pose. R: Prediction-based opportunistic sensing for resilient and efficient sensor networks,” *ACM Trans. Sens. Netw.*, vol. 17, no. 1, pp. 1–41, 2020.
- [5] S. Karaman and E. Frazzoli, “Sampling-based algorithms for optimal motion planning,” *Int. J. Robot. Res.*, vol. 30, no. 7, pp. 846–894, 2011.
- [6] J. Bruce and M. Veloso, “Real-time randomized path planning for robot navigation,” in *IEEE Int. Conf. Intell. Robots Syst.*, vol. 3, 2002, pp. 2383–2388.
- [7] D. Ferguson, N. Kalra, and A. Stentz, “Replanning with RRTs,” in *IEEE Int. Conf. Robot. Automat.*, 2006, pp. 1243–1248.
- [8] M. Zucker, J. Kuffner, and M. Branicky, “Multipartite RRTs for rapid replanning in dynamic environments,” in *IEEE Int. Conf. Robot. Automat.*, 2007, pp. 1603–1609.
- [9] M. Otte and E. Frazzoli, “RRT^X: Asymptotically optimal single-query sampling-based motion planning with quick replanning,” *Int. J. Robot. Res.*, vol. 35, no. 7, pp. 797–822, 2016.
- [10] Y. Chen, Z. He, and S. Li, “Horizon-based lazy optimal RRT for fast, efficient replanning in dynamic environment,” *Auton. Robots*, vol. 43, no. 8, pp. 2271–2292, 2019.
- [11] C. Yuan, G. Liu, W. Zhang, and X. Pan, “An efficient RRT cache method in dynamic environments for path planning,” *Robot. Auton. Syst.*, vol. 131, p. 103595, 2020.
- [12] J. Qi, H. Yang, and H. Sun, “MOD-RRT*: A sampling-based algorithm for robot path planning in dynamic environment,” *IEEE Trans. Ind. Electron.*, vol. 68, no. 8, pp. 7244–7251, Aug. 2021.
- [13] P. Leven and S. Hutchinson, “A framework for real-time path planning in changing environments,” *Int. J. Robot. Res.*, vol. 21, no. 12, pp. 999–1030, 2002.
- [14] S. Koenig and M. Likhachev, “D* Lite,” *Aaai/iaai*, vol. 15, 2002.

[15] S. Koenig, M. Likhachev, and D. Furcy, “Lifelong Planning A*,” *Artificial Intelligence*, vol. 155, no. 1-2, pp. 93–146, 2004.

[16] M. Zucker, N. Ratliff, A. D. Dragan, M. Pivtoraiko, M. Klingensmith, C. M. Dellin, J. A. Bagnell, and S. S. Srinivasa, “CHOMP: Covariant hamiltonian optimization for motion planning,” *Int. J. Robot. Res.*, vol. 32, no. 9-10, pp. 1164–1193, 2013.

[17] D. Hsu, R. Kindel, J.-C. Latombe, and S. Rock, “Randomized kinodynamic motion planning with moving obstacles,” *Int. J. Robot. Res.*, vol. 21, no. 3, pp. 233–255, 2002.

[18] K. Hauser, “On responsiveness, safety, and completeness in real-time motion planning,” *Auton. Robots*, vol. 32, no. 1, pp. 35–48, 2012.

[19] T. Fraichard and H. Asama, “Inevitable collision states—a step towards safer robots?” *Advanced Robotics*, vol. 18, no. 10, pp. 1001–1024, 2004.

[20] J. Snape, J. Van Den Berg, S. J. Guy, and D. Manocha, “The hybrid reciprocal velocity obstacle,” *IEEE Trans. Robot.*, vol. 27, no. 4, pp. 696–706, 2011.

[21] K. Zhu, B. Li, W. Zhe, and T. Zhang, “Collision avoidance among dense heterogeneous agents using deep reinforcement learning,” *IEEE Robot. Automat. Lett.*, vol. 8, no. 1, pp. 57–64, 2022.

[22] T. Fan, P. Long, W. Liu, and J. Pan, “Distributed multi-robot collision avoidance via deep reinforcement learning for navigation in complex scenarios,” *Int. J. Robot. Res.*, vol. 39, no. 7, pp. 856–892, 2020.

[23] [Online]. Available: <https://category.yahboom.net/products>

[24] L. Paull, S. Saeedi, M. Seto, and H. Li, “AUV navigation and localization: A review,” *IEEE J. Ocean. Eng.*, vol. 39, no. 1, pp. 131–149, 2013.

[25] J. L. Fernández, C. Watkins, D. P. Losada, and M. D. Medina, “Evaluating different landmark positioning systems within the ride architecture,” *J. Phys. Agents.*, vol. 7, no. 1, pp. 3–11, 2013.

[26] Y. Bar-Shalom, X. R. Li, and T. Kirubarajan, *Estimation with applications to tracking and navigation: theory algorithms and software*. John Wiley & Sons, 2004.

[27] S. Thrun, W. Burgard, and D. Fox, *Probabilistic robotics*. MIT press, 2005.

[28] K. Mittal, J. Song, S. Gupta, and T. A. Wettergren, “Rapid path planning for dubins vehicles under environmental currents,” *Robot. Auton. Syst.*, vol. 134, p. 103646, 2020.

[29] Z. Shen, J. P. Wilson, and S. Gupta, “An online coverage path planning algorithm for curvature-constrained AUVs,” in *Proc. OCEANS’17 MTS/IEEE*, Seattle, WA, USA, Oct. 2019, pp. 1–5.

[30] J. Song and S. Gupta, “CARE: Cooperative autonomy for resilience and efficiency of robot teams for complete coverage of unknown environments under robot failures,” *Auton. Robots*, vol. 44, pp. 647–671, 2020.

[31] Z. Shen, J. P. Wilson, and S. Gupta, “ ϵ^* +: An online coverage path planning algorithm for energy-constrained autonomous vehicles,” *arXiv preprint arXiv:2008.13041*, 2020.

[32] Z. Shen, J. Song, K. Mittal, and S. Gupta, “CT-CPP: Coverage path planning for 3D terrain reconstruction using dynamic coverage trees,” *IEEE Robot. Automat. Lett.*, vol. 7, no. 1, pp. 135–142, Jan. 2022.

Distribution A. Approved for public release: distribution unlimited. (AFRL-2023-1595) Date Approved 04-06-2023.